Journal of Solid State Chemistry **149,** 180–188 (2000)
Article ID jssc.1999.8520, available online at http://www.idealibrary.com on IDEAL®

Structural Phase Transformations in Crystalline Gallium Orthophosphate

K. Jacobs,* P. Hofmann,* D. Klimm,* J. Reichow,* and M. Schneider†

*Institut für Kristallzüchtung im Forschungsverbund Berlin e.V., Max-Born-Strasse 2, D - 12489 Berlin, Germany; and †ACA—Institut für Angewandte Chemie Berlin-Adlershof e.V., Richard-Willstätter-Strasse 12, D-12489 Berlin, Germany
E-mail: jacobs@ikz-berlin.de

Received August 4, 1999; in revised form September 14, 1999; accepted September 21, 1999

Structural changes proceeding in gallium orthophosphate crystals under thermal treatment have been studied by means of thermoanalytical methods and X-ray diffraction. The samples were characterized with respect to their water content by means of IR absorption. The occurrence of structural changes has been investigated as a function of thermal history, annealing temperature, annealing duration, and cooling rate. Freshly crystallized material shows always the low-quartz analogue modification. During the first heating a transformation into the high-cristobalite form proceeds at about 970°C. This structural change is connected with a weight loss and the emanation of vapor phase species, both indicating the release of water from the samples. Cooling down the high-cristobalite form can lead either to the metastable low-cristobalite or the thermodynamically stable low-quartz modification. The cooling rate is the deciding factor for the occurrence of one or the other phase. The stability range of crystals originally in the low-cristobalite form has been studied by various annealing procedures. It is concluded that the low-quartz structure is thermodynamically stable and can be deliberately obtained between room temperature and about 930°C, while the high-cristobalite modification is stable at higher temperatures. The low-cristobalite form, observed at room temperature nearly without any exception after a first high-temperature treatment, is only metastable. Its occurrence can be suppressed by proper thermal processing. © 2000 Academic Press

Key Words: **gallium orthophosphate; phase transformation; thermal analysis; X-ray diffraction.**

1. INTRODUCTION

Gallium orthophosphate, $GaPO_4$, is a III–V analogue of quartz, with alternating occupation of the Si positions in quartz, Si_2O_4, by Ga and P atoms, respectively. It is a highly promising material for piezoelectric devices (1, 2), although the growth of high-quality, large-sized single crystals is not yet governed satisfactorily.

In comparison to the most widely used crystalline piezoelectric material, quartz, gallium orthophosphate has a stronger piezoelectric effect and higher mechanical coupling constants and Q-values, and it does not show stress-induced twinning. Comparable to quartz, the material possesses temperature-compensated orientations, high electrical resistivity up to high temperatures, and lack of primary pyroelectricity. One of the most attractive properties for the industrial application of $GaPO_4$ is the thermal stability of these properties. The usability of quartz for piezoelectric applications is limited to temperatures below 350°C, above which stress-induced twinning occurs and the piezoelectric coefficient d_{11} strongly decreases. The deterioration of the piezoelectric properties of quartz is due to structural changes. At 573°C a reversible phase transition α-quartz$\leftrightarrow\beta$-quartz occurs. Low quartz, or α-quartz, has a trigonal primitive lattice with $a = 0.491$ nm and $c = 0.540$ nm. Its space group is $P3_221$ or $P3_121$. High quartz, or β-quartz, has essentially the same lattice, with the lattice constants $a = 0.501$ nm and $c = 0.547$ nm; the space group is $P6_122$ or $P6_222$, respectively. The main difference between the two structures is in the placing and orientation of the largely regular SiO_4 tetrahedra (3). The shapes of the tetrahedra, i.e., the bond lengths and the Si–O–Si hinge angles, differ only very slightly. In low quartz, alternate Si atoms are shifted toward the hexad axis and the others are twisted away from it, keeping triad screw symmetry. Moreover, the tetrahedra do not have a diad axis of the tetrahedron parallel to the triad axis of the structure. The space group of high quartz is a supergroup of the low quartz space group.

As mentioned, the $\alpha \rightarrow \beta$ phase transition occurs in quartz at 573°C. In the quartz homeotypic compound berlinite, $AlPO_4$, the same transition is observed at 588°C. It is, however, lacking in $GaPO_4$. The $\alpha\leftrightarrow\beta$ transition in MXO_4 quartz-like materials is discussed from a more general crystallochemical point of view by Philippot *et al.* (4).

The thermal behavior of $GaPO_4$ has been studied by a number of authors (5–12) for both scientific and technical reasons. From the available literature data it must be concluded that the method of $GaPO_4$ preparation, the thermal

0022-4596/00 $35.00
Copyright © 2000 by Academic Press
All rights of reproduction in any form reserved.

history of the crystals, the rates of temperature changes, and, maybe, yet other material properties influence the phase transformations occurring in $GaPO_4$ crystals during thermal treatment.

In this paper, additional data will be presented on structure transformations occurring in $GaPO_4$ crystals when exposed to thermal treatment. The effects of annealing temperature and time, as well as those of the cooling rate, have been studied systematically. Besides X-ray diffraction and differential thermoanalysis, thermogravimetry, mass spectrometry, and IR absorption measurement have also been employed as methods of investigation.

2. EXPERIMENTAL

2.1. Growth of $GaPO_4$ Crystals

In contrast to other investigations, in this study only $GaPO_4$ samples were investigated that had been deliberately prepared in crystal growth experiments. Without foregoing precipitation or recrystallization of solid feed material, saturated solutions were prepared by dissolving metallic Ga in concentrated (85%) H_3PO_4 at about 140°C, up to the formation of a saturated solution. A heater with a seed crystal attached to it was introduced into this clear solution. Due to the retrograde temperature dependence of the solubility, $GaPO_4$ crystals were grown at a constant interface temperature of 140°C on the hotter seed crystal only, without spontaneous nucleation in the solution. The driving force for the growth was the local temperature gradient. A critical problem of the open arrangement was the loss of water from the growth solution. The weight loss due to the evaporation of water was thoroughly determined, and the amount evaporated was added every 2 days. As discussed later, there is some evidence that the properties of the growing crystals will be influenced by their water content. This is usually in the order of 0.2 weight-% in as-grown crystals. It depends on the composition of the feed solution, the growth rate, and the growth temperature. More details on the growth process will be presented elsewhere (13).

2.2. Thermal Analysis

Simultaneous DTA (differential thermoanalytic) and TG (thermogravimetric) measurements were performed using a NETZSCH STA 409C thermoanalytic device with sample carrier HIGH RT 2. Samples with masses between 15 and 50 mg were placed in corundum crucibles for thermal treatment in the range $20°C \leq T \leq 1200°C$. Temperature and enthalpy calibration of the sample carrier were performed prior to the measurements by means of the melting of Zn, Au, and the phase transitions of $BaCO_3$ as reference samples. A furnace with SiC heaters allowed us to perform the DTA/TG measurements in flowing air (50 ml/min). A BALZERS quadrupole mass spectrometer (QMS) is coupled to the DTA equipment via a vitreous carbon "skimmer," which is heated by a second furnace with graphite heaters, thus allowing the simultaneous analysis of the gas emanating during the DTA/TG runs. However, one has to keep in mind that at high temperatures the carbon, which the skimmer is made from, acts as a reducing agent against water and possible decomposition products of $GaPO_4$. Indeed, partial reductive decomposition of the $GaPO_4$ crystals could be observed during long DTA runs (time $t > 5$ h) at high temperatures not performed in air.

2.3. X-Ray Diffraction Measurements

The X-ray powder diffraction measurements were carried out on a STOE STADI P automated transmission diffractometer with Cu$K\alpha_1$ radiation. The X-ray powder diffraction pattern was scanned in the 2θ range 5°–70° (step width 0.5°, 100 s per step) and was recorded with a STOE position-sensitive detector (PSD). The samples were filled in capillaries with 0.5 mm diameter. The phase analysis was carried out with the Visual X^{pow} software package, using the powder diffraction files (PDF) of the International Centre of Diffraction Data.

For the temperature dependent investigations, a GUINIER-LENNÉ (ENRAF-NONIUS) camera was used. Using Cu$K\alpha_1$ radiation the X-ray powder diffraction pattern was scanned at normal atmosphere in a temperature range from room temperature to 1150°C.

2.4. IR Transmission Measurements

IR absorption spectra of a great number of samples were measured by means of a Fourier transform spectrometer BRUKER IFS 66v in the middle infrared region (4000–1000 cm^{-1}). The samples were slabs about 200 μm thick and were prepared by the cutting and polishing of single crystals parallel to their optical axis.

3. RESULTS

3.1. Characterization of Virgin Crystals

All virgin gallium orthophosphate crystals grown as described above show the low-quartz equivalent berlinite structure (in what follows, the "low-quartz" analogue structure will always be denoted by *lQ*, the low-cristobalite equivalent structure by *lC*, and the high-cristobalite equivalent structure by *hC*). No trace of any other structure or any other gallium phosphate could be detected. The crystals are partly clear and partly of milky appearance, but no direct correlation with the infrared absorption could be found.

Typical infrared absorption spectra are seen in Fig. 1. Generally, the crystals show significant absorbtion bands in the OH-stretching region. The absorption spectra of our crystals are essentially identical to those of crystals from

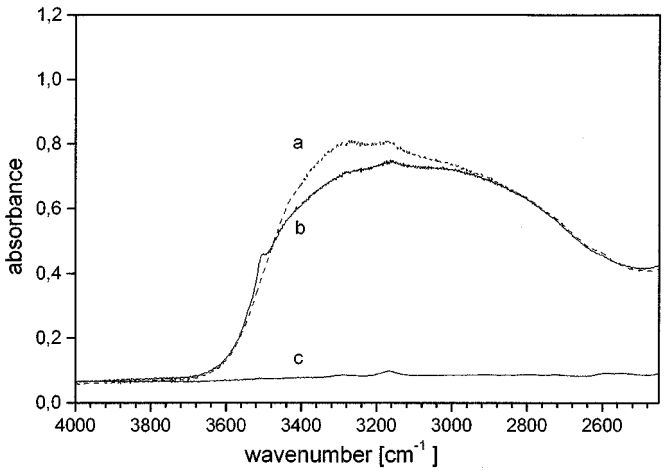

FIG. 1. Infrared absorption of $GaPO_4$ plates: (a) spectrum of a sample with strong OH absorption bands, spectrum taken with $E \parallel c$; (b) spectrum of the same sample as in (a), taken, however, with $E \perp c$; (c) IR absorption spectrum of a sample without significant OH absorption, spectrum taken with $E \perp c$. (E is the electric field vector of the polarized radiation, oriented either parallel or perpendicular to the c axis.)

other groups (14–17). However, there are also crystals without any strong IR absorption, as can also be seen in Fig. 1.

The origin of these absorption bands is not completely clear. Most crystals contain some water. An unambiguous correlation between growth conditions and strength of IR absorption has not been established so far, but more detailed investigations are in progress. A point-wise investigation of a crystal slice by means of an IR microscope with an aperture of 60 μm revealed the water to be rather inhomogeneously incorporated.

3.2. Behavior during First Heating: The lQ → hC Transformation

A crucible filled with as-grown, virgin crystals with *lQ* structure was heated at 10 K/min up to end temperatures in 30°C steps between 900 and 1080°C. Immediately after reaching the maximum temperature, the sample was cooled down to 300°C at 10 K/min and heated again, but up to a final temperature 30°C above, and so on.

No DTA peaks were seen, neither in the heating nor in the cooling phase, in the cycles with the maximum temperatures 900, 930, 960, and 990°C. This held true for the heating up to 1020°C; during cooling from this temperature, however, for the first time a weak exothermic DTA peak appeared at about 580°C. In the subsequent heating cycles an endothermic peak was seen at about 620°C. The exothermic peak at 580°C, observed during cooling, increased in strength in the subsequent runs.

More typical, however, is the observation that virgin samples with the *lQ* structure showed a sharp endothermic peak in differential thermal analysis, DTA, at temperatures around 960°C … 970°C when they were heated for the first time. No other feature was observed up to the maximum temperature of about 1200°C investigated in this study. This peak, however, was no longer observed in subsequent heating cycles.

Interestingly, coinciding with the DTA peak, at the same sharp onset temperature a weight loss was observed, amounting usually to about 0.2–0.5% of the initial mass. Sometimes, this weight loss was still observed to occur during the second heating. In this case, however, it was much weaker. Also connected with the DTA peak, vapor phase species with specific masses $m/z = 2$, 16, 18, and 28 were found to be freed. The occurrence of these species was attributed to the release of water from the $GaPO_4$ crystals. This was reduced by the heated carbon chimney, connecting the mass spectrometer with the DTA head, according to the chemical reactions

$$H_2O_{(g)} + C_{(s)} \leftrightarrow CO_{(g)} + H_{2(g)}$$

and

$$C_{(s)} + 2H_{2(g)} \leftrightarrow CH_{4(g)}.$$

At temperatures around 1000°C, the equilibrium was almost completely shifted to the right-hand side. Therefore, the appearance of carbon monoxide with the relative molecular mass $m/z = 28$ and of methane with $m/z = 16$ was actually due to the release of water. Figure 2 shows the DTA signal, the weight, and the intensity of the $m/z = 28$ signal in mass spectrometry during the first heating process. Neither the weight loss nor the emanation of gases were observed in the case of the sample without OH-absorption bands in the middle IR (cf. Fig. 1).

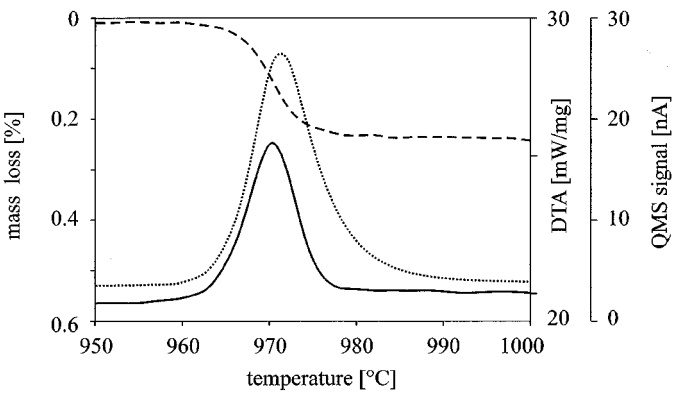

FIG. 2. DTA signal (———), mass loss (---), and abundance of vapor phase species with $m/z = 28$ (CO) (quadrupole mass spectrometer signal QMS, ·····) during the first heating of virgin $GaPO_4$ crystals. At $T \approx 970$°C the transformation $lQ \rightarrow hC$ takes place. At the same time water is released from the sample.

TABLE 1
Literature Data on Structural Phase Transitions in Gallium Orthophosphate Crystals

Author	Process	Temperature (°C)	Sign	Peak characteristics	Transformation	Comments
Perloff, 1956 (5)	1st heating	970 … 980	endothermic	fairly sharp; sometimes broad and shallow and shifted to higher T	$lQ \rightarrow hC$	slow at inversion T; fast at higher T
	1st cooling	around 900	exothermic	wide variations according to those on heating	$hC \rightarrow lQ$	in XRD, seen already at 960°C; complete in a few hours at 950°C; slower at lower T
		574 ± 5	exothermic	always sharp	$hC \rightarrow lC$	very rapid, readily
	2nd heating	618 ± 5	endothermic	always sharp	$lC \rightarrow hC$	reversible
		970 … 990	endothermic			
	2nd cooling			identical to 1st cooling		
Shafer and Roy, 1956 (6)	quenching of 24-h annealed samples	933 ± 4			$Q \rightarrow C$	easily reversible
	heating	616 ± 2			$C \rightarrow (Q)$	
Tananaev and Chudinova, 1964 (20)	1st heating	80–140	endothermic	very broad		loss of water from amorphous $GaPO_4 \cdot 3H_2O$
	1st heating	535–545	exothermic	well distinctive	$amorphous \rightarrow lC$	
	1st heating and cooling (?)	940	endothermic	very sharp	$lC \leftrightarrow hC$	reversible
Cohen and Klement, 1979 (8)	heating	613 ± 4			$lC \rightarrow hC$	DTA signals become increasingly weaker with increasing p, T, and duration of the run
	cooling	557 ± 4			$hC \rightarrow lC$	
Kosten and Arnold, 1980 (9)		933			$lQ \rightarrow hC$	very rapid at $T > 1000$°C
					$hC \rightarrow lQ$	much slower than in opposite direction
	heating	633			$lC \rightarrow hC$	
	cooling	578			$hC \rightarrow lC$	
Cachau-Herreillat, Bennazha, Goiffon, Ibanez, and Philippot, 1992 (12)		933			$lQ \leftrightarrow hC$	
		633			$lC \leftrightarrow hC$	
		574			$hC \leftrightarrow lC$	
Barz, Schneider, and Gille, 1999 (11)	1st heating	970	endothermic	strong and sharp	$lQ \leftrightarrow hC$	
	1st cooling	590	exothermic	strong and sharp	$hC \rightarrow lC$	low kinetic barrier;
	2nd heating	620	endothermic	strong and sharp	$lC \rightarrow hC$	very reproducible; easily reversible
		800	exothermic		$hC \rightarrow lQ$	kinetically hindered; activation energy sufficient at $T > 800$°C
		970	endothermic	strong	$lQ \rightarrow hC$	
	2nd cooling	900	exothermic	weak and broad	$hC \rightarrow lQ$ (partially)	
		590		as in 1st cooling		

Also in the X-ray diffraction pattern, only one structural change was observed to occur during the first heating phase. The first appearance of the new phase, the high-cristobalite equivalent one, *hC*, became visible in X-ray diffraction at temperatures about 40 to 50°C lower than those for the DTA peak and the weight loss, i.e., at about 920°C. No other structural change was observed to occur.

Whereas the behavior during the first heating cycle was always the same for any sample, and was also widely in agreement with all published results (cf. Table 1), the behavior of the samples during further stages of thermal processing depended strongly on absolute temperatures, cooling rates, and annealing times, and also on their thermal history. Therefore, these effects will be discussed separately. The great majority of all samples showed a behavior as shown in Fig. 3 by the DTA signals taken during the first and the second thermal cycling. This behavior is in agreement with the observations of Barz *et al.* (11) as long as the first heating and cooling segments are considered; during the second heating process, however, another behavior was found. The intermediate appearance of the *lQ* phase during the second heating process, observed by Barz *et al.* (11) to occur in the range 800 to 870°C, has never been found in our investigations. A systematic investigation of the effects of various heat treatments should contribute to the clarification of the situation.

3.3. *Effect of Annealing Temperature*

A sample was annealed for 40 h each time at different temperatures $870°C \leq T_{ann} \leq 930°C$. The repeated thermal cycle was as follows: heating at a rate of 10 K/min up to T_{ann}, keeping at T_{ann} for 40 h, cooling down at a rate of -10 K/min to 300°C; heating at 10 K/min up to 1200°C (in order to reestablish a well-defined starting condition) and cooling to RT at -10 K/min. DTA measurements were performed during the heating and cooling phases before and after the annealing period and during the heating phase leading to a final temperature of 1200°C.

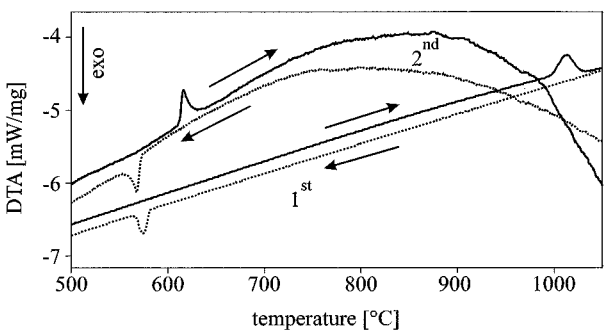

FIG. 3. DTA signal recorded during the first and second heating/cooling cycles. The starting material in the first heating/cooling cycle is the *lQ* modification, while it is the *lC* modification in the second cycle. The reversible $hC \leftrightarrow lC$ transformation appears at $\approx 580°C$ during cooling and at $\approx 620°C$ upon heating.

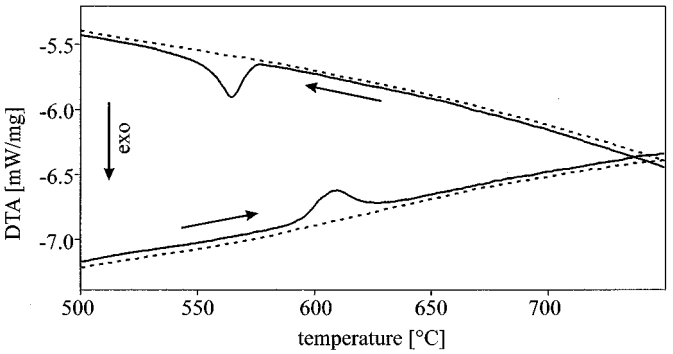

FIG. 4. DTA signals from originally *lC* samples, obtained during cooling and heating periods, immediately following a 40-h annealing period at 925°C (····) or 930°C (—). At the lower annealing temperature the *lQ* phase is formed; therefore, the $lC \leftrightarrow hC$ transition can not be observed during cooling and reheating.

Cooling from 1200°C at -10 K/min led in any case to the *lC* phase at room temperature, which was then the starting point for the next annealing experiments. The following results were obtained:

During any heating an endothermic peak appeared at 620°C. This corresponds to the $lC \rightarrow hC$ transformation.

After annealing, a distinct behavior has been observed for samples annealed at 870, 885, 900, 915, 920, and 925°C, on the one hand, and samples annealed at 930°C and above, on the other hand. This becomes evident in Fig. 4, which shows the DTA signals taken during the heating and cooling cycles following the annealing phases at 925 or 930°C, respectively.

No DTA peak was observed during the cooling of the samples annealed at temperatures $T_{ann} < 930°C$. In this group of samples, annealed at lower temperatures, during the subsequent heating from 300 to 1200°C only one broad and flat endothermic DTA peak appeared, with its maximum at about 1050°C. The commonly expected endothermic peak at about 620°C for the $lC \rightarrow hC$ transformation was not seen. During the subsequent cooling from 1200°C, the exothermic $hC \rightarrow lC$ transition was observed at 560°C.

In contrast to these results, a beautiful exothermic peak appeared at 560°C when the sample annealed at 930°C was cooled down. The only peak observed in the subsequent heating period up to 1200°C was the one at 620°C. The broad peak around 1050°C, observed even in the sample annealed at 925°C, was lacking.

The result of a further annealing experiment shall be added here: Another sample was heated to 1200°C at a rate of 3.2 K/min. It was annealed at $T_{ann} = 1200°C$ for 2 h and cooled to room temperature with a mean rate of -22 K/min in the interval between 1200 and 1120°C and

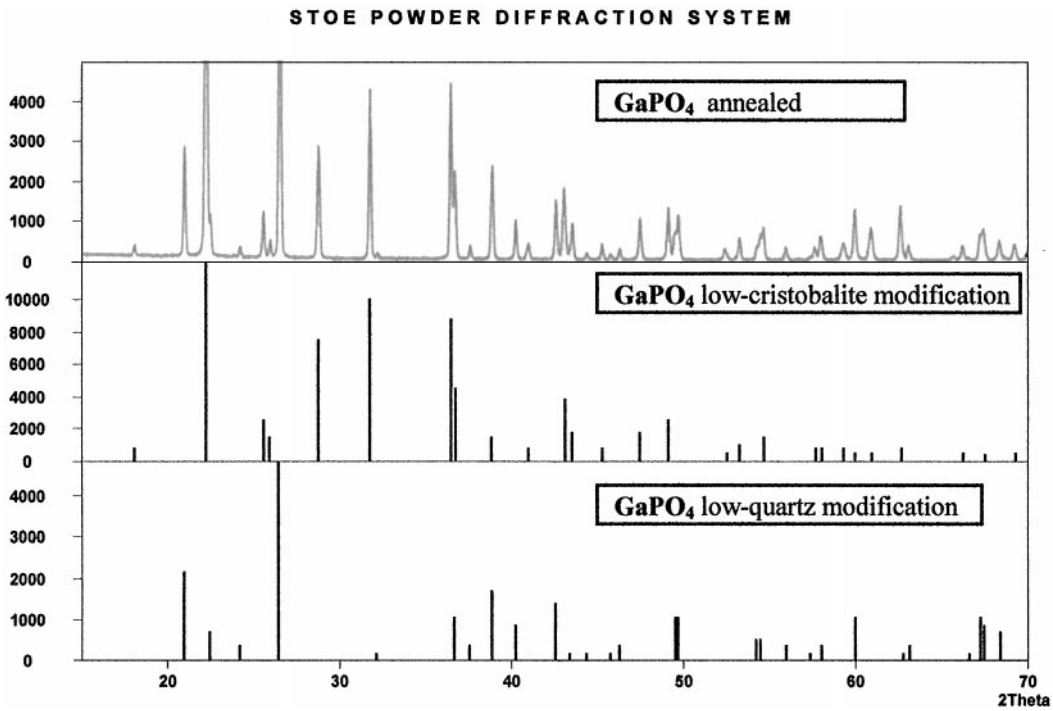

FIG. 5. X-ray diffraction pattern of a sample annealed for 2 h at 1200°C and cooled slowly (see text for details). Also shown are the powder diffraction files from the International Centre of Diffraction Data. Annealing under these conditions leads to a mixture of the *lQ* and the *lC* modifications.

of -2 K/min between 1100 and 950°C. The cooling rate became still slower with time. The X-ray diffraction diagram taken at room temperature (Fig. 5) shows a mixture of the *lQ* and the *lC* modifications.

3.4. *Effect of Annealing Duration*

The results presented in the previous section made it interesting to study the effect of annealing duration at 930°C and one lower temperature by DTA. The same charge as in the DTA experiments described in the preceding section has been investigated. The thermal cycling was similar to that described above; i.e., heating and cooling rates were 10 K/min and the original *lC* structure was regenerated by heating up to 1200°C after each annealing and cooling segment.

First the sample was annealed at 915°C for 3, 5, 7, 10, 15, 20, and 40 h. When the sample cooled down from the annealing temperature $T_{ann} = 915$°C a distinct behavior was observed, depending on the annealing duration. When the sample with *lC*-type structure was annealed for a shorter duration only, up to 7 h inclusive, the DTA peak at 560°C, ascribed to the $hC \rightarrow lC$ transformation, was seen during cooling from T_{ann}. Longer annealing, 10 h or more, caused the $hC \rightarrow lC$ transformation peak to disappear. In accordance with this observation, the endothermic $lC \rightarrow hC$ transition at 620°C was observed during reheating of the samples annealed for shorter times only. These results are shown in Fig. 6 by the different DTA signals obtained from the same sample but annealed at 915°C for 5, 10 h, respectively.

3.5. *Effect of Cooling Rate*

Temperature-dependent X-ray diffraction measurements clearly revealed the significance of the cooling rate. A sample was heated from room temperature to 1115°C

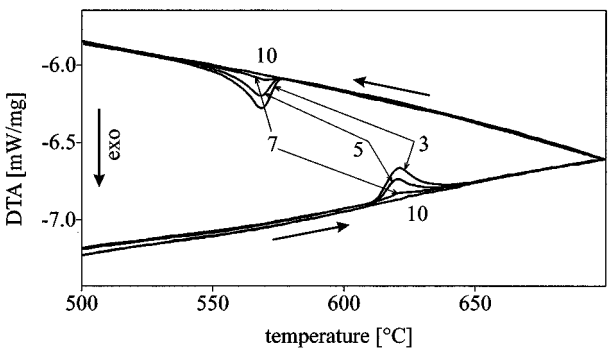

FIG. 6. DTA signals from a sample annealed at 915°C. The numbers denote the annealing duration in hours. Only longer annealing brings about a mostly complete transformation $hC \rightarrow lQ$; i.e., the $lC \leftrightarrow hC$ transition is no longer observed.

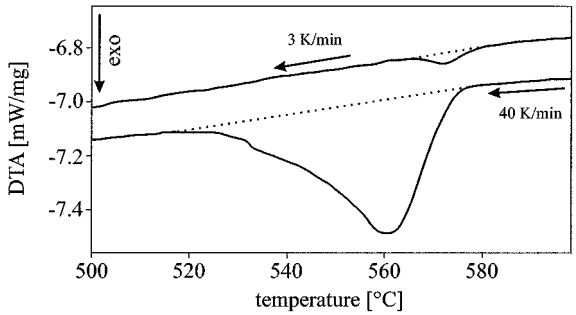

FIG. 7. Effect of cooling rate on the phase transformations. The sample was linearly cooled from 1115°C (*hC* state) (a) − 3 K/min or (b) − 40 K/min. X-ray diffraction shows that slow cooling results in the *lQ*-modification at room temperature, while fast cooling leads to the *lC* modification.

with a linear heating rate of 3 K/min. As usual, the transformation $lQ \rightarrow hC$ was observed with the onset at about 910°C. During cooling from 1115°C back to room temperature at a rate of − 3 K/min, the X-ray diffraction pattern showed the back-transformation $hC \rightarrow lQ$ proceeding to completeness within the temperature interval 860 … 850°C.

During the subsequent second heating cycle at 5 K/min up to 920°C, only the lattice expansion, but no structure transformations was seen. In this case the starting situation was different from that in all the experiments described before: The second heating started from the *lQ* phase, not from the *lC* modification. Twenty hours of annealing at 920°C did not cause any structural change. Also, during the subsequent second cooling at − 2.5 K/min down to room temperature no change was seen.

The next heating cycle was identical to the first one, in terms of both conditions and observations. The cool-down was performed from 1115°C to room temperature within 40 min. The temperature dropped very fast within the first minute by 215 to 900°C; after two minutes the temperature was 760°C, and 660°C was reached after 3 min. Then, the X-ray diffraction pattern taken at room temperature revealed that only the *lC* phase was present.

The DTA signal recorded in the course of a nearly identical thermal treatment is shown in Fig. 7. During slow cooling, performed at a cooling rate of − 3 K/min, only a rather weak DTA peak (peak area: − 5.3 J/g) evolved with an onset temperature of about 580°C. In contrast, fast cooling − 40 K/min resulted in a distinct exothermic DTA peak (peak area: − 29.9 J/g) with about the same onset temperature. This again is the well-known $hC \rightarrow lC$ transition.

4. DISCUSSION

4.1. Results from the Literature

The earliest investigation of the structural changes occurring in gallium orthophosphate under thermal treatment was published in 1956. Perloff (5) found that $GaPO_4$ has structures analogous to the low-quartz, low-cristobalite, and high-cristobalite types of silica. No evidence was found for the occurrence of a high-quartz form or of tridymite structures. These results were essentially confirmed by Shafer and Roy (6), although only one form of quartz and one of cristobalite are mentioned in their paper. Cohen and Klement (8) studied the pressure dependence of the high↔low cristobalite transition in SiO_2, $AlPO_4$, and $GaPO_4$. Extrapolation to 1 bar yielded transformation temperatures of 613°C on heating and 557°C on cooling. These results may be compared with the data of Leadbetter *et al.* (7), 595° to 645°C on heating and 605 to 540°C on cooling. Cachau-Herreillat *et al.* (13) report that the $lC \rightarrow hC$ transition occured at 633°C, while the reversal was observed at 574°C. X-ray investigations by high-temperature Guinier methods were performed by Kosten and Arnold (9). They came to the same findings as Perloff (5). Also, the displacing transformation in the cristobalite form was confirmed with a hysteresis of 55 K and a volume change connected with this transformation of 6%. These authors pointed out that a marked difference of $GaPO_4$ in comparison to SiO_2 and $AlPO_4$ was the velocity of the reconstructive transformation between the quartz and the cristobalite forms. On heating, the transformation proceeded quickly at temperatures above 975°C, while it proceeded slowly in the opposite direction. Above 560°C within several hours, detectable amounts of the quartz form evolved from the cristobalite form. Similar results were mentioned by Perloff (5), who could detect traces of the *lQ* form after 6 days of annealing of the *lC* form at 560°C. Also, Barz *et al.* (11) attributed a sometimes observed additional exothermic DTA peak at about 900°C during the second cooling period to a partial transformation of the *hC* phase into the *lQ* modification. X-ray powder diffraction measurements showed the transition of the *hC* form into both the *lQ* and the *lC* phases when the samples were cooled down from 1100°C to room temperature at a rate of 5 K/min. Annealing the samples at 950°C for 12 h led to an almost complete transformation into the *lQ* modification. Perloff attributed the inability to detect the thermodynamically stable *lQ* modification after cooling to the smallness of the powder grains.

The observations published in the literature up to now are summarized in Table 1.

4.2. Interpretation of the Experimental Results of This Study

Gallium orthophosphate grown from phosphoric acid solutions crystallizes without any exceptions in the *lQ*-modification. This structure is retained as long as the sample has not seen temperatures higher than about 970°C. At around this temperature, generally the transition

$lQ \rightarrow hC$ becomes visible in the DTA. There is a rather wide scatter in the temperature at which this transition occurs. In the X-ray diffraction patterns, the first appearance of the hC phase is observed at about 920°C. It has to be mentioned that in the XRD investigations a rather slow heating rate has been applied. Furthermore, powders from very small crystallites are used in XRD, while the crystallites investigated in the thermoanalytic investigations are larger. The DTA signal is in most cases a sharp peak at temperatures around 970°C. Obviously, with increasing heating rates the $lQ \rightarrow hC$ transformation is shifted to higher temperatures. Therefore, an appropriate expression for the relationship between heating rate and time (or temperature of phase transition) could be derived by considering the required activation energy for the phase transition: For the phase transition to occur a certain activation energy $E_{lQ \rightarrow hC}$ must be supplied. The rate of transformation $r_{lQ \rightarrow hC}$ can be expected to follow an expression of the form

$$r_{lQ \rightarrow hC} = r^* \exp\left(-\frac{E_{lQ \rightarrow hC}}{kT}\right) = r^* \exp\left(-\frac{E_{lQ \rightarrow hC}}{k\left(\frac{dT}{dt}\right)\Delta t}\right),$$

with

r^* as a constant
k as the Boltzmann constant,
$\left(\frac{dT}{dt}\right)$ as the heating rate, and
Δt as the time of heating above a certain characteristic temperature T^*, $\Delta t = t - t_{T^*}$.

Sometimes, the transformation proceeds rather slowly over a certain wider temperature range. In such cases no clear DTA peak is observed. Doubtless, however, the transformation has taken place because the $hC \rightarrow lC$ transition is seen in the cooling period at temperatures of about 570 … 580°C.

An interesting new observation is that a weight loss occurs at exactly the same temperature at which the DTA peak for the $lQ \rightarrow hC$ transition appears. The detection of H_2 and CO is a clear indication that the weight loss is due to the evaporation of water. In one sample, without significant IR absorption by OH-groups, neither any weight loss nor the DTA signal indicating the $lQ \rightarrow hC$ transition were observed. During cooling, however, also in this sample, the well-known DTA peak for the $hC \rightarrow lC$ transition appeared at about 550°C.

Thus, on heating a sample, in any case the $lQ \rightarrow hC$ transformation proceeds, independent of whether it contains water or not. This transition has a relative high kinetic barrier. Therefore, the transition temperature is not well defined. The lowest temperature for the transition we have ever seen was about 915°C, the highest temperature was about 1000°C. Most frequently, however, this phase transformation becomes evident in DTA at temperatures around 970°C. When the sample contains water, it is released when the phase transition occurs. Both the structural transformation and the evaporation of water are endothermic; therefore, the DTA peak is more distinct in such samples. Probably, the water content lowers the kinetic barrier for the $lQ \rightarrow hC$ transformation. Also a thermodynamic explanation could apply: During the heat treatment, a supersaturation of water dissolved in the crystals is generated. The pressure in bubbles, containing the water, increases extremely. Releasing this supersaturation lowers the Gibbs free energy of the crystal. This can provide energy for the endothermic transformation into the hC form. Similar arguments have been applied for the formation of dislocations in water-containing berlinite crystals (19). Thus, besides the effects of grain size and heating rate, the different water content of the samples can also be responsible for the rather wide range in which the $lQ \rightarrow hC$ transformation temperature has been found by ourselves and other authors.

In an early Russian publication (20), the results of thermoanalytical investigations of a $GaPO_4 \cdot 3H_2O$ sample were reported. According to this paper, drying at about 200°C caused a loss in weight of about 24.4–24.8%, which is just equivalent to the loss of the three molecules of water. No further loss in weight was observed on heating to 1000°C.

The modification existing at room temperature, i.e., either the lC or the lQ structure, can be deliberately controlled by appropriate annealing and cooling conditions, provided the sample has undergone, in its thermal history, at least one transformation into the hC modification.

Commonly, as all of the literature results so far presented show, the $GaPO_4$ is found in the lC modification at room temperature after cooling from the hC phase. Thorough investigations, however, show that it can also be obtained exclusively in the lQ modification. This was accomplished by Barz *et al.* (11) by 75 min of annealing at 820°C. From our annealing experiments at different temperatures it can be concluded that the hC modification undergoes a slow phase transition into the lQ modification during annealing at temperatures between 870 and 925°C. During cooling to room temperature this modification remains conserved. When the annealing temperature T_{ann} is $930°C \leq T_{ann} \leq 970°C$, the transformation $hC \rightarrow lQ$ does not take place; the hC modification remains conserved. This means that the lQ modification is no longer stable at temperatures above 925°C.

An important experimental parameter that has not been taken into account in former investigations is the cooling rate. Slow cooling from the hC phase leads to the lQ modification, while fast cooling inevitably results in the lC form. An absolute value for a critical cooling rate can not yet be given. More quantitative investigations remain to be performed in the future.

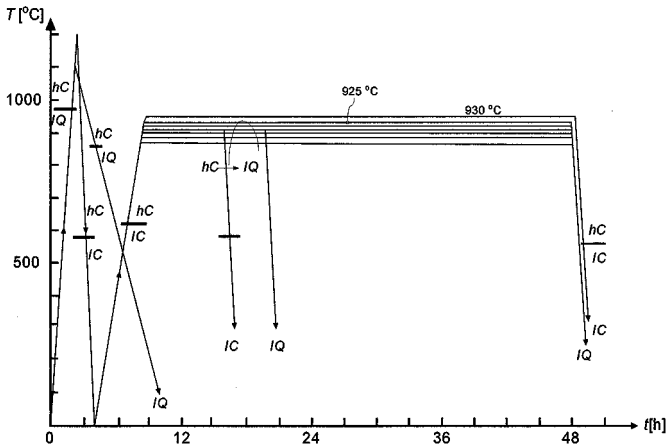

FIG. 8. Compilation of the experiments and the main observations of this study. The horizontal bars show the transition temperatures observed in DTA. The transition from the *hC* modification to the *lQ* form occurring during annealing at temperatures up to 925°C, but no longer at 930°C, can not be seen in a DTA signal. More than 7 h of annealing are required for the transition to proceed to such an extent that the X-ray diffraction pattern is essentially that of the low-quartz analogue modification.

Most of the investigations and their main results are compiled in Fig. 8. Summarizing all the experimental results from this study and the literature, we believe that the *lC* modification is metastable under any conditions; i.e., cooling the *hC* modification of $GaPO_4$ does not proceed via the sequence $hC \rightarrow lC \rightarrow lQ$; instead of this it follows either the path $hC \rightarrow lC_{(\text{metastable})}$ or the path $hC \rightarrow lQ_{(\text{stable})}$. The thermodynamically stable *lQ*-analogue modification is formed below 930°C provided the cooling rate is slow enough (less than 5 K/min). Annealing of the *hC* modification at temperatures below 930°C also leads to the conversion $hC \rightarrow lQ$. Thus, our investigations confirm the tentative stability diagram of Barz *et al.* (11).

5. SUMMARY

The phase transformations proceeding in gallium orthophosphate under thermal treatment have been studied by means of thermal analysis and X-ray diffraction. Furthermore, the samples were characterized with respect to their water content by means of IR absorption. The phase transitions that occur have been studied as a result of annealing temperature, annealing time, and cooling rate. There is clear evidence that the water content of the samples also plays a significant role in the kinetics. The only thermodynamically stable phases existing in the temperature range between room temperature and 1150°C are the low-quartz analogue and the high-cristobalite analogue. The former is stable up to temperatures of about 930°C. This temperature is about 70°C below that estimated by Barz *et al.* (11). During the first heating of the samples, the transition from the *lQ* modification into the *hC* form occurs at temperatures of about 970°C. Absolutely coinciding with this phase transformation, water is released from the material. The water content of the samples seems to lower the kinetic barrier for the phase transformation $lQ \rightarrow hC$. The cooling rate is of primary importance for the transformation of the *hC* phase upon cooling. Low cooling rates (smaller than -5 K/min) enable the $hC \rightarrow lQ$ transition to occur, while higher cooling rates lead to the metastable *lC* modification. Quantitative investigations of the kinetics of the phase conversions are planned.

ACKNOWLEDGMENTS

Thanks are due to Mr. H. Gleichmann from the Innovent e.V. Jena, who supplied one $GaPO_4$ sample with low IR absorption. This work has been performed by means of grant FKZ 03N1031/2 from the German Federal Ministry of Education and Research (BMBF).

REFERENCES

1. P. Krempl, G. Schleinzer, and W. Wallnöfer, *Sensors Actuators A* **61,** 361 (1997).
2. P. W. Krempl, F. Krispel, and W. Wallnöfer, *Ann. Chim. Sci. Mater.* **22,** 623 (1997).
3. H. D. Megaw, "Crystal Structures: A Working Approach." Saunders, Philadelphia/London/Toronto, 1973.
4. E. Philippot, A. Goiffon, A. Ibanez, and M. Pintard, *J. Solid State Chem.* **110,** 356 (1994).
5. A. Perloff, *J. Am. Ceram. Soc.* **39,** 83 (1956).
6. E. S. Shafer and R. Roy *J. Am. Ceram. Soc.* **39,** 330 (1956).
7. A. J. Leadbetter, P. A. Phillips, and A. Wright, *Phil. Mag.* **34,** 453 (1976).
8. L. H. Cohen and W. Klement, Jr., *Phil. Mag. A* **39,** 399 (1979).
9. K. Kosten and H. Arnold, *Z. Kristallogr.* **152,** 119 (1980).
10. E. Philippot, D. Palmier, M. Pintard, and A. Goiffon, *J. Solid State Chem.* **123,** 1 (1996).
11. R.-U. Barz, J. Schneider, and P. Gille, *Z. Kristallogr.* in press.
12. D. Cachau-Herreillat, J. Bennazha, A. Goiffon, A. Ibanez, and E. Philippot, *Eur. J. Solid State Inorg. Chem.* **29,** 1295 (1992).
13. J. Reichow and K. Jacobs, in preparation.
14. F. Krispel, P.W. Krempl, P. Knoll, and W. Wallnöfer, in "Proceedings, 11th Eur. Freq. and Time Forum," p. 233, 1997.
15. E. Philippot, A. Ibanez, A. Goiffon, A. Zarka, J. Schwartzel, and J. Détaint, "Proceedings 1992 International IEEE Freq. Control Symp.," p. 744, 1992.
16. M. Cochez, A. Ibanez, A. Goiffon, and E. Philippot, *Eur. J. Solid State Inorg. Chem.* **30,** 509 (1993).
17. E. Philippot, A. Goiffon, M. Cochez, A. Zarka, B. Capelle, J. Schwartzel, and J. Détaint, *J. Crystal Growth* **130,** 195 (1993).
18. D. Palmier, A. Goiffon, B. Capelle, J. Détaint, and E. Philippot, *J. Crystal Growth* **166,** 347 (1996).
19. J. C. Jumas, A. Goiffon, B. Capelle, A. Zarka, J. C. Doukhan, J. Schwartzel, J. Détaint,, and E. Philippot, *J. Crystal Growth* **80,** 133 (1987).
20. I. V. Tananaev and N. N. Chudinova, *Russ. J. Inorg. Chem.* **9,** 135 (1964).